Polish Society of Composite Materials
Polskie Towarzystwo Materiałów Kompozytowych

22: 3 (2022) 135-141

COMPOSITES THEORY AND PRACTICE
ISSN: 2084-6096
ISSN (online): 2299-128X

B.L.N. Krishna Sai, Pankaj Tambe*

School of Mechanical Engineering, VIT-AP University, Amravati – 522237, Andhra Pradesh, India
**Corresponding author. E-mail: pankaj.tambe@vitap.ac.in*

Received (Otrzymano) 24.01.2022

SCRATCH BEHAVIOUR OF SURFACE MODIFIED HOLLOW GLASS MICROSPHERE FILLED PC/ABS COMPOSITES

In this paper, hollow glass microspheres (HGMs) were surface treated using a silane coupling agent to coat the surface with an amine functional group. Modified and unmodified HGM filled polycarbonate (PC)/acrylonitrile butadiene styrene (ABS) (70/30 wt.%) composites were prepared using a twin-screw extruder and then injection moulding. By means of FTIR spectroscopy, it was found that the modified HGMs containing the amine group formed an aminolysis compound with the PC phase. Scratch studies were performed at low load to avoid fracturing the composites during the test so that deformation of the material only happened in order to understand the influence of HGMs and modified HGM on the scratch behaviour of the composites. The silane modified HGM filled PC70/ABS30 composites exhibited improvement in scratch behaviour as compared to the composites containing unmodified HGMs. The 5 wt.% HGM-NH_2 filled PC70/ABS30 composites demonstrate good improvement in scratch resistance as they attained the the highest values of scratch force, coefficient of friction, and scratch hardness among all the compositions of composites.

Keywords: polycarbonate (PC), normal load, hollow glass microspheres (HGMs), scratch, blend

INTRODUCTION

Polymer blends are sought-after materials in the automobile industry due to their various advantages in terms of properties and cost. The blend of PC/ABS is one of the widely used materials in the automobile industry [1, 2]. The scratch behaviour of the PC/ABS blend is an important area to study with regard to its applications [3-6]. The scratching process is carried by applying a force using a hard tip over the soft polymer, and moving the tip tangentially over the surface at a particular velocity due to which penetration of the polymer by the tip results in mechanical deformation [6]. The scratch properties of materials are determined by the damage created by the hard tip on the material surface by taking the forces between the contact area of the hard tip and polymer material into consideration [7]. Bowden and Tabor et al. [8] explain that the hard tip is moved forward by pushing the material like a wave but not removing it and the measurements depend on the geometry and speed of the hard tip. The scratch on polymer is also dependent on different parameters such as normal load, as well as thermal and stiffness properties of the scratching device [6]. The polymer material when interacting with another body undergoes different types of deformations such as brittle or plastic, based on the angle of the indenter tip. Brittle fracture makes the surface more uneven and more severe damage occurs to the polymer material when compared to plastic deformation [9]. Briscoe et al. [10] studied scratching maps in which the scratch hardness and frictional forces correlated with the deformation mechanism that occurred during scratching.

There have been many studies about the scratch behaviour of PC based composites [11-19]. Arribas et al. [12] studied a polycarbonate/organoclay nanohybrid and reported that the residual depth remains constant after repeated scratches because of strain hardening. The increase in the normal load has shown strain hardening to occur with a lower number of scratches. Bermúdez et al. [17] studied the scratch resistance of pure PC and PC/ZnO nanoparticles processed by injection moulding based on the scratch direction. It shows that the penetration depth is greater in the direction of melt injection flow than the transversal direction for pure PC. On the other hand, the PC/ZnO nanocomposite exhibits a reduction in the penetration depth and an increase the residual depth in the longitudinal direction. Recently, HGMs have also been gaining attention from researchers as a reinforcing filler in PC/ABS blend composites [20]. HGMs are readily available on a large scale and their use in polymer matrices is important in terms of sustainability and environmental concerns with material weight reduction. In addition, the scratch behaviour of PC/ABS blends have not been studied extensively [5]. The blend of PC/ABS is available commercially and using HGMs as a filler in it adds value in terms of improving the mechanical properties.

In this work, HGMs are used as filler material and were surface-modified using a silane coupling agent. Modified and unmodified HGMs were added to a PC70/ABS30 blend to create composites using a twin-screw extruder, followed by injection moulding. The content of modified and unmodified HGMs was varied from 1-5 wt.% in the PC70/ABS30 blend and a comparison was made among them in order to study the scratch properties.

EXPERIMENTAL PART

Materials

Makrolon 2807 PC was procured from Convestro, Germany. The PC has a melt flow rate of 9 cm^3/10 min at the temperature of 300°C with a 1.2 kg load. Terluran GP-22 ABS was procured from Ineos Styrolution Korea Ltd. ABS has a melt flow rate of 19 cm^3/10 min at a temperature of 220°C with a 10 kg load. Ethanol was used as the solvent (Changshu Hongsheng Fine Chemical Co. Ltd, China). Hydrochloric acid (HCL), 3-Aminopropyltriethoxysilane (APTES), and n-propylamine were obtained from SD Fine Chemicals Ltd, India. The HGMs were purchased from 3^M India, India having a density of 0.5 g/cm^3. The composition of the HGMs is borosilicate glass.

Surface treatment of HGM

HGM surface modification using a silane coupling agent involves two types of reactions. The first reaction involves hydroxylation and the second reaction is related to salinization. First, in a round bottom flask 20 ml of concentrated HCl and 180 ml of distilled water were mixed, followed by the addition of 10 g of HGM. The mixture was stirred using a magnetic stirrer for a period of 1 h at the temperature of 90°C for chemical attachment of hydroxyl groups on the HGM surface. After the completion of mixing, the HGMs were removed from the HCL solution and washed with purified water. Next, the HGMs were vacuum dried at 70°C for 8 h to remove moisture. Afterwards, these dried microspheres were again dispersed in 300 ml of a solution of ethanol, 3-aminopropyltriethoxysilane, n-propylamine and were mixed with a magnetic stirrer for 1 h at 60°C. The HGMs were removed from the solution and firstly washed with ethanol and then thoroughly with distilled water. The obtained HGMs were vacuum dried at 80°C for 24 h. Finally, the obtained product is HGM-NH_2.

PC/ABS composite production

Modified and unmodified HGM filled PC70/ABS30 composites were prepared using a twin-screw extruder. The twin-screw extruder supplied by Aasabi Machinery Pvt. Ltd., India having a 25 mm screw diameter and length to diameter (L/D) ratio of 30:1 was used for the work. The twin-screw extruder runs at temperatures between 225-235-250-260°C in four chambers at a 60-rpm screw rotation. The content of unmodified HGMs and modified HGMs was varied from 1 to 5 wt.% in the PC70/ABS30 composites. Samples were prepared for testing the composites using an IM-D30 injection molding machine supplied by Deesha Impex, India. The modified and unmodified HGM filled PC70/ABS30 composites were moulded using injection molding at 245-250-250-260°C and applied high pressure (8 bar) to make the mixture flow into the mould cavity. A sample of the PC/ABS blend without HGMs was also produced for reference.

Characterization

FTIR spectroscopic analysis of HGMs and modified HGMs was performed with an FTIR-4200 by JASCO in the scanning range of 400-4000 cm^{-1} and resolution of 1 cm^{-1}. The HGM surface was examined using a scanning electron microscope (SEM) by Carl Zeiss, Germany, and Apreo2 SEM, Thermofisher Scientific, USA. Scratch testing was performed on all samples of the PC 70/ABS 30 blend and its composites using a scratch tester by DUCOM, Bangalore, India. The test was performed over a scratch length of 10 mm at the scratch speed of 1 mm/min using a diamond indenter. The normal loads were varied from 20 to 40 N for the scratch test for the PC 70/ABS 30 blend and its composite samples.

RESULTS AND DISCUSSION

Characterization of HGM and surface modified HGM

The as-received HGMs were characterized using FTIR spectroscopy and SEM. Figure 1a shows the SEM micrograph of the as-received HGMs. The micrograph shows that the diameter of HGMs lies in the 10-50 μm range. Figure 2a presents the FTIR spectra of the HGMs. It is interesting to note the peak at 469 cm^{-1}, corresponding to the O-Si-O bond of HGMs. Furthermore, the Si-O group of HGMs stretches symmetrically and asymmetrically as demonstrated by the peaks at 795 cm^{-1} and at 1054 cm^{-1}. At 3427 cm^{-1} there is another peak, indicative of stretching vibrations of the –OH group. This observation shows that the main elements in the composition of the as-received HGMs contains an SiO_2 functional group along with an –OH group. The reason for the presence of the –OH group is the moisture absorption over the surface of HGMs. In Figure 2a, the FTIR spectra of the NH_2 modified HGMs show a peak at 1386 cm^{-1}, which indicates the presence of an amine group for HGM-NH_2. Figure 2b presents the peak at 3486 cm^{-1} for N-H stretching, while the peak at 1643 cm^{-1} for N-H bending. In Figure 2b, for the HGM-NH_2 filled PC70/ABS30 composites there is a peak at 1657 cm^{-1}, which is related to the presence of an aminolysis compound [20].

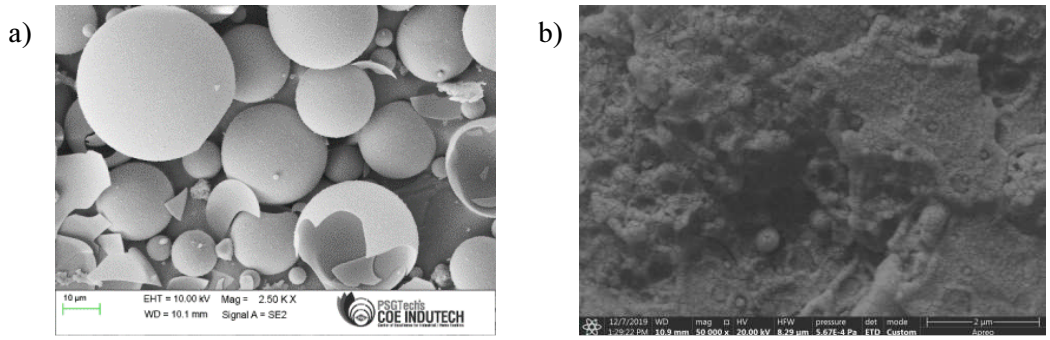

Fig. 1. SEM micrographs of HGM

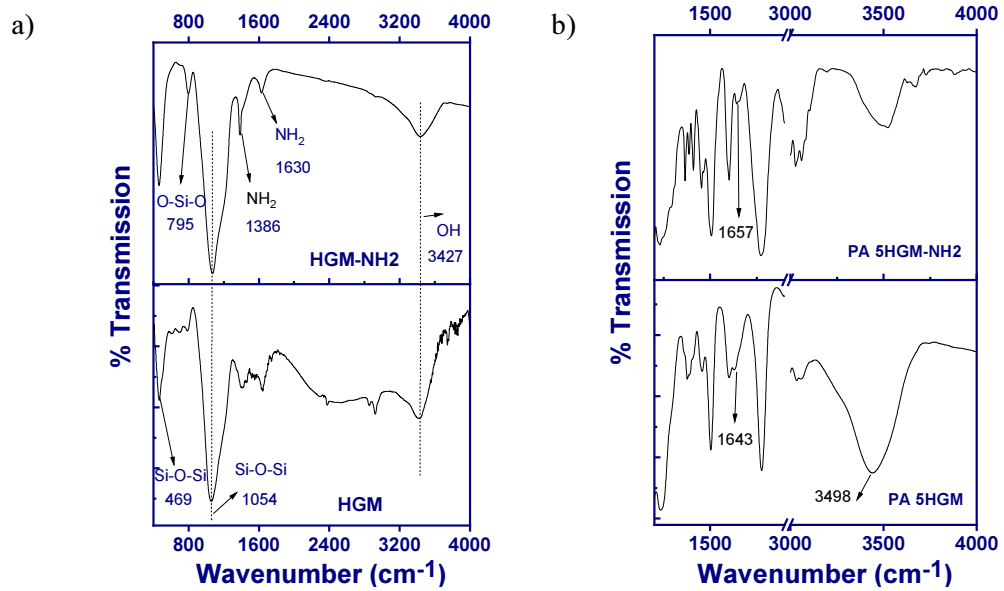

Fig. 2. FTIR spectra of (a) HGM and NH_2 modified HGM (b) HGM filled PC70/ABS30 composites

Scratch behaviour PC70/ABS30 blend and modified and unmodified HGM filled composites

Figure 1b presents the SEM micrograph of the HGM filled PC70/ABS30 composite showing the formation of matrix-droplet morphology with disperse HGMs. In this work, a single scratch was made at a lower load so that the contact pressure results in viscoelastic deformation of the material under study, which causes the formation of a groove. In addition, the contact area of the indenter and polymer has three elements, i.e. the adhesion junction, shear strength of the polymer, and real area of contact [21]. When the indenter slides over the polymer specimens, the specimens and indenter have their respective surface roughness and the peaks of the surface with a certain height are referred to as asperities that are in contact with each other [22]. The indenter hard asperities in contact with the polymer soft asperities form an adhesion junction, resulting in the penetration of the hard asperities with the soft asperities manifesting ploughing or deformation resistance along the real surface area of contact [21, 22]. Figure 3a shows the scratching force as a function of scratch length for the HGM filled PC70/ABS30 composites.

The pure PC70/ABS30 blend exhibits a fluctuating scratch force till a 5 mm scratch length, thereafter the scratching force remained constant with minimal fluctuations. There are two reasons for the fluctuations in force: the first one is due to the adhesive contact resistance of the two dissimilar materials in contact. The second reason is the dissipation of the flexible ABS polymer and the PC phase of the specimens due to viscoelastic losses. It is well known that a transfer layer is formed at the interface of the contact surface due to the cohesion of polymer to the indenter material, which is responsible for sliding at the interface and results in a dissipation of energy [22]. Therefore, after a 5-mm scratch length, the dissipation of energy due to sliding at the interface of the PC70/ABS30 blend and indenter results in a scratch force measurement with minimal fluctuations. With this observation, it is clear that the major reason for the scratch resistance is the ploughing resistance of the PC70/ABS30 material. Figure 3b shows the influence of varied normal load between 20 to 40 N on the scratching behaviour of the HGM filled PC70/ABS30 composites. It shows that the scratching force increases with a varied normal load between 20 to 40 N for the PC70/ABS30 blend. The penetration width and depth can be used to probe the reason for the in-

crease in scratching force value for the PC70/ABS30 blend with an increase in load. The width of the scratch on viscoelastic recovered specimens was measured after scratch testing using a light microscope micrograph and a software tool. The scratch width values increase with increasing normal load. The obtained scratch width values are used to calculate the depth developed during scratching, having geometric consideration of 120° apex angle (α). The depth (h) can be calculated using the following equation:

$$h = \frac{d}{2\,tan\theta} \tag{1}$$

$$\theta = \frac{1}{2}(180 - \alpha) \tag{2}$$

where d is the scratch width, θ is calculated by substituting the apex angle in Equation (2). The depth values are calculated by inserting the θ value in Equation (1) for all the composites.

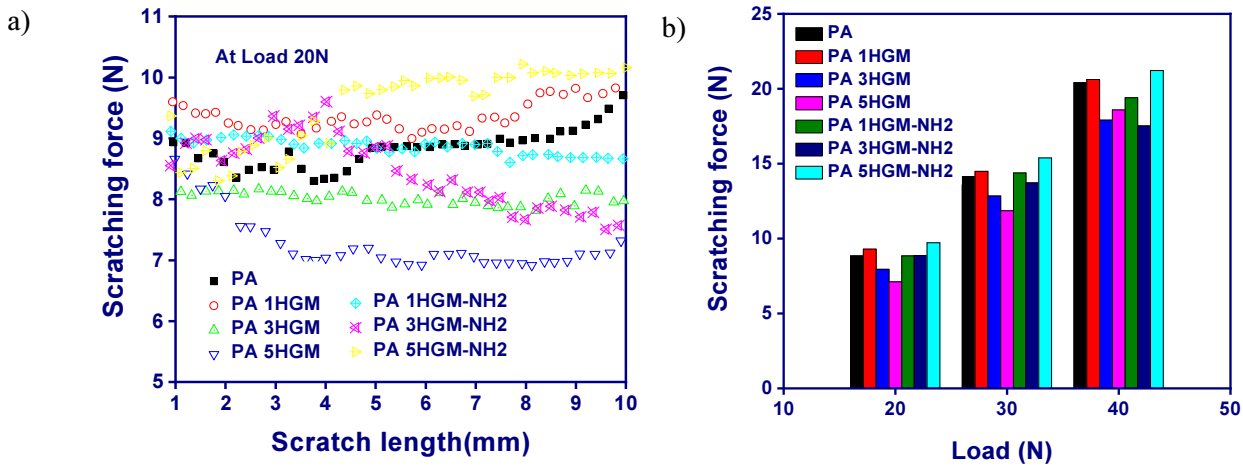

Fig. 3. Scratching force (a) with varied length at 20 N load (b) with varied normal loads of PC70/ABS30 composites

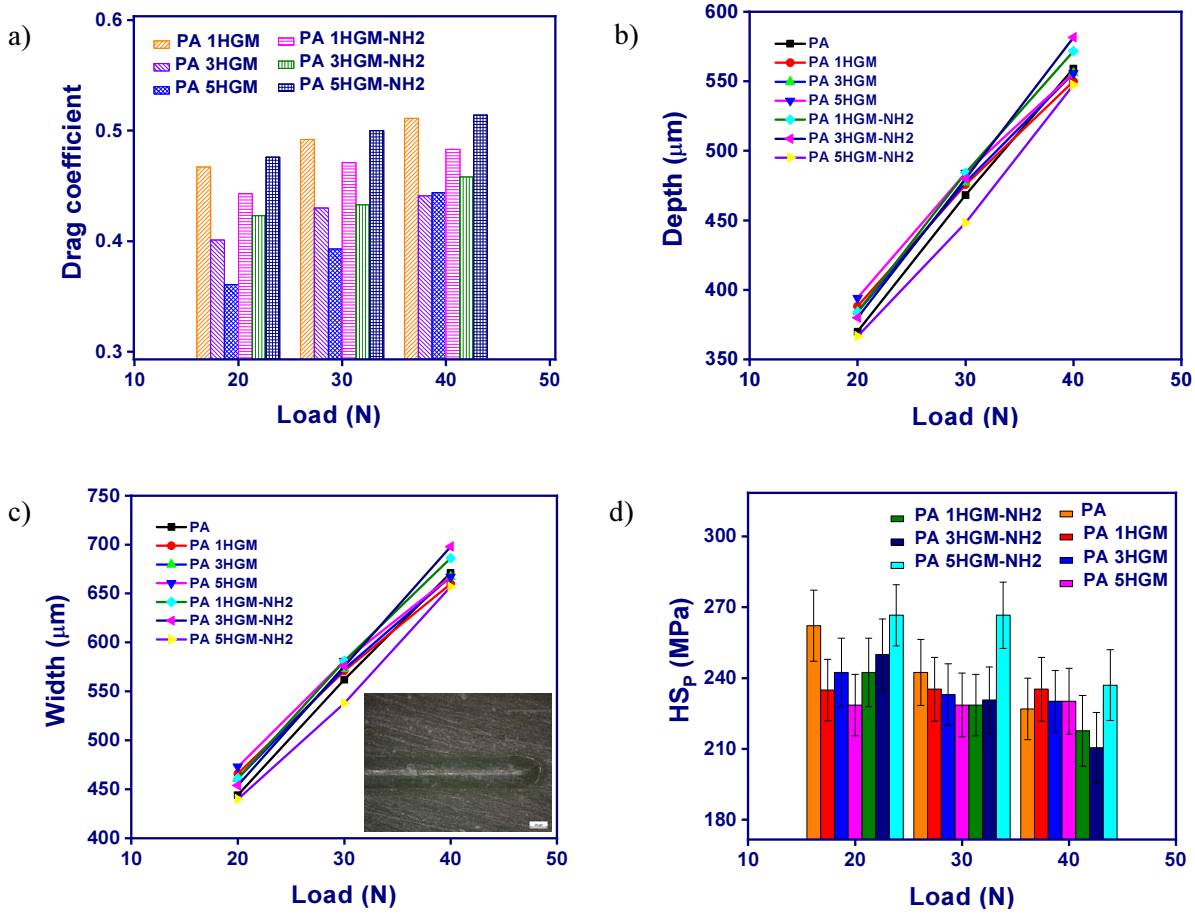

Fig. 4. Drag coefficient (a), depth (b), representative light microscope micrograph (c), scratch hardness (d), of PC70/ABS30 blend and its composites

Figure 4c shows the width of the scratches on the specimens with a representative light microscope micrograph insert, while Figure 4d presents the calculated depth of the scratch with varied normal loads for the PC70/ABS30 material as well as all the composites with the modified and unmodified HGMs. Figure 4d shows that for the PC70/ABS30 material, the depth of the scratch increases with an increase in applied load with scratching. This resulted in a large area of contact between the indenter and PC70/ABS30 material manifesting in more deformation of the material and thus the scratching force values are higher. The scratch width values were again used to calculate the values of scratch hardness. The scratch hardness number (HS_P) is the ratio of applied normal force on the moving stylus by the projected area of scratching contact. HS_P can be determined by means of the following formula:

$$HS_P = \frac{8P}{\pi d^2} \tag{3}$$

where: P – normal force and d – scratch width. The scratch hardness values are calculated by using equation (3). Figure 4d shows the HS_P value with a varied normal load of the pure blend, modified and unmodified HGM filled PC70/ABS30 composites. At the 20 N normal load, the HS_P value of the PC70/ABS30 blend is 262.2 MPa. The HS_P value for the PC70/ABS30 material decreases with an increase in load as the depth of indentation increases, which results in an increase in scratch width.

Figure 3a presents the scratching force as a function of scratch length for the PC70/ABS30 blend and its composites. The scratching force for the 1 wt.% HGM filled PC70/ABS30 composite shows a marginal increase along the scratch length associated with uniform dispersion of HGMs. The 3 and 5 wt.% of HGM filled PC70/ABS30 composites exhibited a decrease in scratching force along the scratch length due to the aggregation of HGM in the PC70/ABS30 matrix. Figure 3b presents the scratching force as a function of normal load for the HGM filled PC70/ABS30 composites. From Figure 3b, it was observed that the measured scratch force values rise with increasing normal load for the HGM filled PC70/ABS30 composites. At the 20 N load, the pure PC70/ABS30 blend has a scratch force value of 8.83 N. With the addition of 1 wt.% HGM to the PC70/ABS30 material there was an increase in the scratch force value to 9.3 N. A further addition of 3 and 5 wt.% HGM to PC70/ABS30 results in a decrease in the scratch force values to 7.95 N and 7.10 N because of the agglomeration of HGM in the PC70/ABS30 matrix.

These observations of scratch force can be confirmed with the help of calculating the stylus drag coefficient (D_{sc}). The stylus drag coefficient (D_{sc}) can be defined as F_{scr}/P, where: F_{scr} = average scratching force along the length of the scratch, and P = normal force on the stylus. The importance of D_{sc} is the resistance of the test surface to the scratch indenter. Figure 4a presents the drag coefficient as a function of load for the HGM filled PC70/ABS30 composites with varying normal loads from 20 to 40 N. From Figure 4a, it is observed that the calculated drag coefficient values grow with increasing normal load for the composites. At the 20 N load, the PC70/ABS30 material containing 1 wt.% HGM has drag coefficient values of 0.467, whereas with the addition of 3 and 5 wt.% HGMs to the PC70/ABS30 matrix decreases in of the drag coefficient value to 0.401 and 0.361, respectively were observed. Thus, due to the aggregation of HGMs, the drag coefficient is lower for the 3 and 5 wt.% HGMs in the PC70/ABS30 matrix, which results in lower scratching force values. Figure 4b presents the depth of the scratch with varied normal loads for the HGM filled PC70/ABS30 composites. At the 20 N normal load, it is observed that the pure PC70/ABS30 blend has a scratch depth value of 370 μm. With the addition of 1 wt.% HGM to the PC70/ABS30 material, an increase in the calculated depth value to 388 μm as compared to the pure blend was observed. Furthermore, the addition of 3 wt.% HGMs to the PC70/ABS30 matrix shows a depth value to 384 μm. With the addition of 5 wt.% HGMs to the PC70/ABS30 matrix, has the greatest depth value as compared to the 1 and 3 wt.% HGM filled PC70/ABS30 composites and the pure blend. The depth values are higher owing to the lower resistance to scratching load, and thus the HS_P values are lower for the HGM filled PC70/ABS30 composite as compared to the neat material (Fig. 4d). The increase in depth results in an increase in the width of the scratch.

To increase the dispersion of filler in the polymer matrix, the surface of the HGMs was modified. The influence of HGM-NH_2 on the PC70/ABS30 material is as follows. Figure 3a shows the scratching force as a function of scratch length for the HGM-NH_2 filled PC70/ABS30 composites. The measured value of scratching force at the 5-mm scratch distance for the HGM-NH_2 filled PC70/ABS30composites is shown in Figure 3b. With the addition of 1 and 3 wt.% HGM-NH_2 to the PC70/ABS30 material, the scratch force values are 8.84 and 8.85, which are higher values as compared to 3, 5 wt.% HGM filled PC70/ABS30 composites and the pure PC70/ABS30 blend. Finally, the addition of 5 wt.% HGM-NH_2 to PC70/ABS30 results in a measured scratch force value of 9.70 N, which is the highest value compared to all the modified and unmodified HGM filled PC70/ABS30 composites. At the 30 and 40 N load, a similar behaviour as the 20 N load was also observed with respect to the 5 wt.% HGM-NH_2 filled PC70/ABS30 composites as it exhibits the highest scratch force values as compared to all the modified and unmodified HGM filled PC70/ABS30 composites. The improvement in the scratch force values for the modified HGM filled PC70/ABS30 composites due to surface modification of the filler im-

proves the dispersion of the HGM filler by reducing the agglomerative clusters in the polymer matrix [23, 24] and also due to interaction between the C=O group of the polycarbonate and functional groups in the modified HGM. Because of this interaction, the polycarbonate chain exhibits more resistance to scratching force. This can be further understood from the drag coefficient values of the HGM-NH_2 filled PC70/ABS30 composites, which are shown in Figure 4a. The HGM-NH_2 filled PC70/ABS30 composites exhibit higher drag coefficient values as compared to the HGM filled PC70/ABS30 composites, indicating the role of the interfacial modification of the filler and matrix. From the results presented in Figure 4b, it is observed that at all the varied normal loads, the 5 wt.% HGM-NH_2 filled PC70/ABS30 composites have the lowest scratch depth and width values as compared to all the composites due to the fact that surface modification of HGMs increases the polymer-filler interaction, which in turn, improves the resistance to scratch indentation. The HS_P values for the modified HGM filled PC70/ABS30 composites were also calculated for the 20 N load. The addition of 1 wt.% HGM-NH_2 to the PC70/ABS30 material shows an increase in the HS_P value to 242 MPa as compared to the 1 wt.% HGM filled PC70/ABS30 blends. A further addition of 3 wt.% HGM-NH_2 to the PC70/ABS30 matrix results in a rise in the HS_P value to 250 MPa in comparison to the 3 wt.% HGM filled PC70/ABS30 composites, but it is low comparing to the neat PC70/ABS30 material. Finally, the addition of 5 wt.% HGM-NH_2 to the PC70/ABS30 matrix effects the highest HS_P value as compared to all the PC70/ABS30 composites. A similar observation was noted for the HS_P values of the HGM-NH_2 filled PC70/ABS30 composites at other applied loads. Thus, from the above discussion, the 5 wt.% HGM-NH_2 composite has more amine functional groups, and its melt reaction with the PC phase influences the surface properties of the PC70/ABS30 composites.

Coefficient of scratch resistance of modified and unmodified HGM filled PC70/ABS30 composites

The ratio of the tangential force to normal force of the stylus is the coefficient of scratch resistance (μ_{scr}). Figure 5a shows μ_{scr} as a function of scratch length and Figure 5b for μ_{scr} as a function of normal load for modified and unmodified HGM filled PC70/ABS30 composites. These values are compared with a varied load between 20 to 40 N and noted at a 5-mm scratch length. From Figure 5b, it was observed that the obtained μ_{scr} values grow with an increasing normal load for all the modified and unmodified HGM filled PC70/ABS30 composites. At the 20 N load, the pure PC70/ABS30 blend attained a μ_{scr} value of 0.442. The addition of 1 wt.% HGM to the PC70/ABS30 material resulted in an increase in the μ_{scr} value to 0.466. Further additions of 3 and 5 wt.% HGM to the PC70/ABS30 matrix showed a decrease in the μ_{scr} values to 0.398 and 0.354 due to agglomeration of the HGM filler, which leads to reduction in scratch resistance.

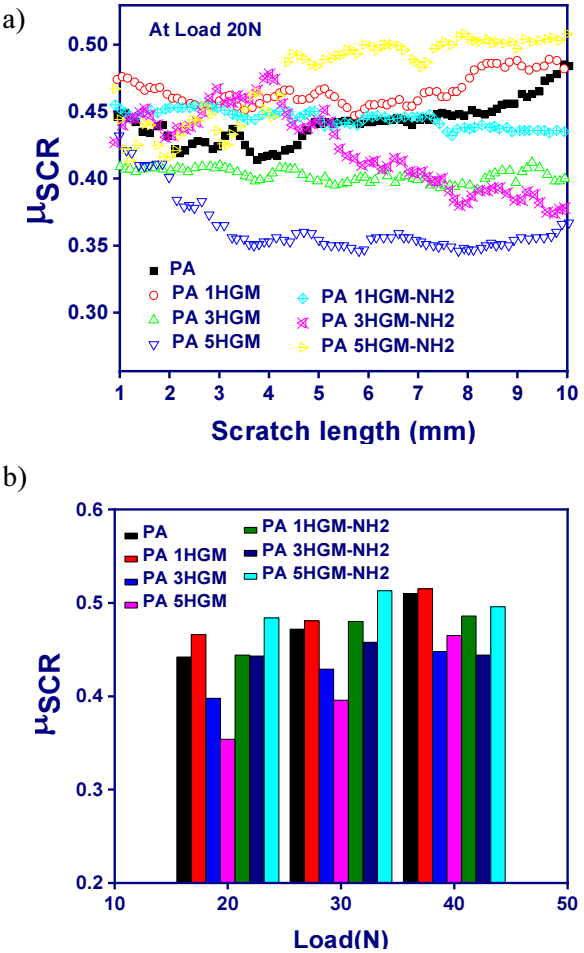

Fig. 5. Coefficient of scratch resistance (a) with varied length at 20 N load (b) with varied normal loads on PC70/ABS30 blend and its composites

The addition of 1 and 3 wt.% HGM-NH_2 to the PC70/ABS30 material had the effect of μ_{scr} values of 0.444 and 0.443, which are higher as compared to the 3, 5 wt.% HGM filled PC70/ABS30 composites and the pure PC70/ABS30 blend. When comparing the 1 and 3 wt.% HGM-NH_2 filled composites, the 3 wt.% HGM-NH_2 filled composites show slightly lower μ_{scr} values due to agglomerates of HGMs but owing to modification of the filler material the μ_{scr} variation was reduced. Moreover, the 5 wt.% HGM-NH_2 filled PC70/ABS30 composite reached a μ_{scr} value of 0.484, which is higher compared to all the modified and unmodified HGM filled PC70/ABS30 composites and the neat matrix material. It is thanks to the formation of the aminolysis compound, which restricts the chain deformation, resulting in the μ_{scr} values being the highest for the 5 wt.% HGM-NH_2 filled PC70/ABS30 composites. At higher applied loads during the scratch test, the μ_{scr} values did not change significantly and showed an increase in the μ_{scr} values owing to the increased area of contact for the respective compositions.

CONCLUSIONS

In this work, HGMs were surface modified using a silane coupling agent and characterized using FTIR spectroscopy. The modified HGMs containing an amine group on the surface react with the PC phase to form an aminolysis compound. Scratch studies were carried out at a low load to prevent fracture and a scratch formation occurs due to the deformation in order to understand the influence of HGMs and modified HGMs on the scratch behaviour of the PC70/ABS30 blend and its composites. The scratch formed a groove. The scratching force values decrease with an increase in the content of HGMs in the PC70/ABS30 composites due to inadequate interfacial adhesion between the HGMs and the PC phase. This influenced the scratch depth, width, HS_P and μ_{scr} values of the HGM filled PC70/ABS30 composites. Furthermore, the addition of HGM-NH_2 to the PC70/ABS30 material results in an increase in the scratching force at the 5 wt.% HGM-NH_2 content owing to the lower scratch depth because of resistance offered by the aminolysis compound and better dispersion of HGM-NH_2 in the PC70/ABS30 matrix. In addition, the HS_P and μ_{scr} values of the HGM-NH_2 filled PC70/ABS30 composites were the highest.

REFERENCES

[1] Bärwinkel S., Seidel A., Hobeika S., Hufen R., Mörl M., Altstädt V., Morphology formation in PC/ABS blends during thermal processing and the effect of the viscosity ratio of blend partners, Materials 2016, 9(8), 659, DOI: 10.3390/ma9080659.

[2] Orzan E., Janewithayapun R., Gutkin R., Lo Re G., Kallio K., Thermo-mechanical variability of post-industrial and post-consumer recyclate PC-ABS, Polymer Testing 2021, 99, 107216, DOI: 10.1016/j.polymertesting.2021.107216.

[3] Sushmita K., Madras G., Bose S., The journey of polycarbonate-based composites towards suppressing electromagnetic radiation, Functional Composite Materials 2021, 2(1), DOI: 10.1186/s42252-021-00025-1.

[4] Seo J.S., Jeon H.T., Han T.H., Rheological investigation of relaxation behavior of polycarbonate/acrylonitrile-butadiene-styrene blends, Polymers 2020, 12(9), 1916, DOI: 10.3390/polym12091916.

[5] Nishino K., Shindo Y., Takayama T., Ito H., Improvement of impact strength and hydrolytic stability of PC/ABS blend using reactive polymer, Journal of Applied Polymer Science 2016, 134(9), DOI: 10.1002/app.44550.

[6] Jiang H., Browning R., Sue H.J., Understanding of scratch-induced damage mechanisms in polymers, Polymer 2009, 50(16), 4056-4065, DOI: 10.1016/j.polymer.2009.06.061.

[7] Gauthier C., Lafaye S., Schirrer R., Elastic recovery of a scratch in a polymeric surface: Experiments and analysis, Tribology International 2001, 34(7), 469-479, DOI: 10.1016/s0301-679x(01)00043-3.

[8] Bowden F.P., Tabor D., The Friction and Lubrication of Solids, Oxford University Press, 1951.

[9] Briscoe B.J., Pelillo E., Sinha S.K., Characterisation of the scratch deformation mechanisms for poly (methylmethacrylate) using surface optical reflectivity, Polymer International 1997, 43(4), 359-367, DOI: 10.1002/(sici)1097-0126(199708)43:4<359::aid-pi772>3.0.co;2-c.

[10] Briscoe B.J., Evans P.D., Pellilo E., Sinha S.K., Scratching maps for polymers, Wear 1996, 200(1-2), 137-147, DOI: 10.1016/s0043-1648(96)07314-0.

[11] Khun N.W., Liu E., Thermal, mechanical and tribological properties of polycarbonate/acrylonitrile-butadiene-styrene blends, Journal of Polymer Engineering 2013, 33(6), 535--543, DOI: 10.1515/polyeng-2013-0039.

[12] Arribas A., Bermudez M.D., Brostow W., Carrion-Vilches F.J., Olea-Mejia O., Scratch resistance of a polycarbonate + organoclay nanohybrid, Express Polymer Letters 2009, 3(10), 621-629, DOI: 10.3144/expresspolymlett.2009.78.

[13] Boentoro W., Pflug A., Szyszka B., Scratch resistance analysis of coatings on glass and polycarbonate, Thin Solid Films 2009, 517(10), 3121-3125, DOI: 10.1016/j.tsf.2008.11.119.

[14] Wang Z.Z., Gu P., Zhang Z., Indentation and scratch behavior of nano-sio2/polycarbonate composite coating at the micro/nano-scale, Wear 2010, 269(1-2), 21-25, DOI: 10.1016/j.wear.2010.03.003.

[15] Liu J., Jiang H., Cheng Q., Wang C., Investigation of nano-scale scratch and stick-slip behaviors of polycarbonate using atomic force microscopy, Tribology International 2018, 125, 59-65, DOI: 10.1016/j.triboint.2018.04.024.

[16] Fabbri P., Messori M., Toselli M., Veronesi P., Rocha J., Pilati F., Enhancing the scratch resistance of polycarbonate with poly(ethylene oxide)-silica hybrid coatings, Advances in Polymer Technology 2009, 27(2), 117-126, DOI: 10.1002/adv.20122.

[17] Bermúdez M.D., Brostow W., Carrión-Vilches F.J., Sanes J., Scratch resistance of polycarbonate containing ZnO nanoparticles: Effects of sliding direction, Journal of Nanoscience and Nanotechnology 2010, 10(10), 6683--6689, DOI: 10.1166/jnn.2010.2513.

[18] Wee J.W., Park S.Y., Choi B.H., Observation and understanding of scratch behaviors of glass fiber reinforced polycarbonate plates with various packing pressures during the injection molding process, Tribology International 2015, 90, 491-501, DOI: 10.1016/j.triboint.2015.05.009.

[19] Jang K.S., Low-density polycarbonate composites with robust hollow glass microspheres by tailorable processing variables, Polymer Testing 2020, 84, 106408, DOI: 10.1016/j.polymertesting.2020.106408.

[20] Sai B.L., Tambe P., Surface modified hollow glass microsphere reinforced 70/30 (wt/wt) P.C/A.B.S blends: Influence on Rheological, mechanical, and thermo-mechanical properties, Composite Interfaces 2021, 1-25, DOI: 10.1080/09276440.2021.1986974.

[21] Friedrich K., Friction and Wear of Polymer Composites, Composite Materials Series, Vol. 1, Elsevier, 1986.

[22] Myshkin N.K., Kovalev A.V., Adhesion and Friction of Polymers, Polymer Tribology, Imperial Press, 2009.

[23] Vignali A., Iannace S., Falcone G., Utzeri R., Stagnaro P., Bertini F., Lightweight poly(ε-caprolactone) composites with surface modified hollow glass microspheres for use in rotational molding: Thermal, rheological and mechanical properties, Polymers 2019, 11(4), 624, DOI: 10.3390/polym11040624.

[24] Li R., Wang P., Zhang P., Fan G., Wang G., Ouyang X., Ma N., Wei H., Surface modification of hollow glass microsphere and its marine-adaptive composites with epoxy resin, Advanced Composites Letters 2020, 29, DOI: 10.1177/2633366x20974682.

